Journal of Fluorescence (2022) 32:1073–1087
https://doi.org/10.1007/s10895-022-02917-2

ORIGINAL ARTICLE

# New Insights into Optoelectronic Features of Eu(III) Complexes with Heterocyclic Ligand for Advanced Optical Applications

**Manisha Bedi[1] · Pooja Chhillar[1] · Priyanka Dhankhar[1] · Jyoti Khanagwal[2] · V. B. Taxak · S. P. Khatkar[1] · Priti Boora Doon[1]**

Received: 22 December 2021 / Accepted: 25 February 2022 / Published online: 18 March 2022


## Abstract

Our present technological society needs the assistance of lanthanide luminescence in almost every field to meet the global energy demands. In present research work we have synthesized five (one binary and four ternary) 5-(4-methylphenyl)-2-furoic acid based Eu(III) complexes with ancillary ligands, namely, aqua ($H_2O$), neocuproine (neo), 2, 2'-bipyridyl (bipy), bathophenanthroline (batho) and 1, 10-phenanthroline (phen). The spectroscopic analysis and photophysical features are characterized by the use of different investigative techniques. All the findings obtained from EDAX, elemental (CHN) analysis, FT-IR, NMR, UV–visible spectroscopy declared the coordination of ligand binding sites with the europium ion. These Eu(III) complexes possess good thermal stability and excellent optoelectronic features as predicted with the help of TGA and PL analysis. Diffuse reflectance spectral studies confirm their applications in the wide band gap semiconductors. The Judd–Ofelt analysis and monoexponential behavior of lifetime reveals the existence of asymmetric and single local environment around europium ion. All the complexes show sharp red emission validated by CIE color coordinates, color purity, asymmetric ratio and CCT values. SEM analysis tells that the bulk of these complexes comprised of spherical shaped particles with uniform distribution.

**Keywords** Europium ion · Emission · Luminescence · Ancillary ligand · Energy transfer

## Abbreviations

| | |
|---|---|
| DMSO | Dimethylsulphoxide, |
| WBGs | Wide-band gap semiconductors |
| eV | Electron Volt |
| $\tau$ | Decay time |
| $I_0$ and I | Luminescence intensities at time 0 and t, |
| MHz | Megahertz |
| °C | Degree Celsius |
| °C/min | Degree Celsius per minute |
| mmol | Millimol |
| mL | Milliliter |
| $F(R_\infty)$ | Kubelka–Munk function, |
| C | Constant of proportionality |
| % | Percentage |
| S | Scattering coefficient, |
| K | Absorption coefficient, |
| $\nu$ | Frequency |
| $\delta$ | Chemical shift on delta scale |
| $\Delta E_0$ | Energy gap between excited singlet and triplet state |
| $\Delta E_1$ | Energy gap between excited triplet state and resonating level |
| nm | Nanometer |
| $S_0$ | Ground singlet, |
| $S_1$ | Excited singlet state, |
| $T_1$ | Excited triplet state |
| KBr | Potassium bromide |
| x and y | Color coordinates of sample, |
| ppm | Parts per million |
| OLEDs | Organic light emitting diodes |
| µg/mL | Microgram per milliliter |
| mmol/L | Millimol per liter |
| phen | 1,10- Phenanthroline, |
| batho | Bathophenanthroline |
| bipy | 2,2- Bipyridyl |
| $Eu^{3+}$ | Trivalent europium ion |
| Gd | Gadolinium metal |

✉ Priti Boora Doon
pritiboora@gmail.com

[1] Department of Chemistry, Maharshi Dayanand University, Rohtak-124001, India

[2] Department of Chemistry, Government College for Women, Bhiwani-127021, India

| | |
|---|---|
| CHN | Carbon, Hydrogen, Nitrogen, |
| DR | Diffuse reflectance |
| $E_g$ | Band-gap energy |
| $^1$H-NMR | Proton nuclear magnetic resonance, |
| h | Planck' constant |
| PL | Photoluminescence, |
| FT-IR | Fourier transform infra-red, |
| TG and DTG | Thermal and differential thermogravimetric |
| $^1$H-NMR | Proton nuclear magnetic resonance |
| UV–vis | Ultraviolet–visible |
| CIE | Commission International de I'Eclairage |
| OLEDs | Organic light emitting diodes |

## Introduction

Recent trends in science and technology reflects the interest of researchers in solving fascinating puzzles dealing with lanthanide luminescence. In the view of data published in recent researches, the selected theme of "lanthanide luminescence" opens the new door of opportunities for innovation in field of light emitting materials [1–6]. The optical properties of lanthanide ions attract keen attention due to their pure color emission in desired visible region. The electronic configuration of lanthanide ions possesses variety of well defined energy levels as 4f orbitals are screened by 5s and 5 p sub-shells. One of the landmarks in the electronic features is the presence of sharp and easily recognizable 4f-4f transitions resulted into fixed line like emission. As f-f transitions are not Laporte permitted since they have to follow selection rule results into low molar absorption coefficient. Consequently, bare lanthanide ion is unable to achieve high emission intensity by direct excitation. Intensified lanthanide mediated luminescence can be accomplished by choosing an alternative approach i.e. introduction of organic functionalized ligands [7–10]. These organic moieties have possible light harvesting sites, large molar absorption coefficient and sensitize the metal ion by antenna effect. The organic ligand also safeguards the excited states of metal ion from nonradiative deactivation [11]. Moreover, an appropriate design of ligand could enhance emission intensity, luminescence lifetime and chromaticity. Hence these metal organic complexes generates a large interest as an emissive material in many fields of medicinal and biological analysis as well as in light emitting diodes (LEDs) [12–16].

Any lanthanide ion can be used as a luminescent probe, but some ions possess unique features ($Eu^{3+}$), which enlighten their preferential use. Keeping in mind its narrow line like metal-centered intense luminescence, the Eu (III) ion is considered as most suitable luminescent probe. The bright red luminescence of these metal organic complexes is due to ($^5D_0$-$^7F_2$) ED transition and its modified intensity is subjected to the composition and symmetry of coordination sphere. Another way of benefitting luminosity is the incorporation of asymmetry in coordination sphere by addition of ancillary ligands with the organic ones [17–19]. An additional advantage of ancillary ligands is the reduction in vibrational deactivation produced by O–H and C-H bonds which reduces emission intensity and luminescence lifetime. Hence these ancillary ligands perform well in fulfilling the coordination number and also tuned the photophysical properties by synergistic effect [20–23].

In an effort toward the design of metal organic complexes several classes of organic functionalized ligands are tested and fortunately, 5-(4-methyl phenyl) furoic acid (MPFA) is selected for the synthesis. This heterocyclic derivative acts as good complexing antenna as it possesses strong possible coordination sites. In this work, we present synthesis and characterization of five metal organic complexes using 5-(4-methyl phenyl) furoic acid (MPFA) as primary ligand and aqua ($H_2O$), neocuproine (neo), 2, 2-bipyridyl (bipy), bathophenanthroline (batho) and 1, 10-phenantharoline (phen) as ancillary ligands. The general formulas of complexes are $Eu(MPFA)_3.H_2O$ (C1), $Eu(MPFA)_3$neo (C2), $EuMPFA)_3$bipy (C3), $Eu(MPFA)_3$batho (C4), $Eu(MPFA)_3$phen (C5). All the metal organic complexes are characterized by employing various investigative techniques such as elemental analysis (CHN), energy dispersive X-ray spectroscopy (EDAX), Infrared (IR) spectroscopy, thermal gravimetric analysis (TGA), and nuclear magnetic resonance spectroscopy (NMR). The photoluminescent behavior is analyzed by UV–visible absorption (UV), diffused reflectance (DR) and photoluminescence spectroscopy (PL).

## Experimental Section

### Materials and Apparatus

Europium nitrate ($Eu(NO_3)0.5H_2O$, 99.9%) and 5-(4-methyl phenyl) furoic acid (MPFA) are the common starting material for the synthesis and are purchased from Sigma Aldrich. All the measurements are accomplished at room temperature. The percentage of europium ion is calculated by employing complexometric titration with EDTA solution. The percentage composition of the elements (C, H, N) present in the complexes is estimated on a "Perkin Elmer 2400 CHN Elemental Analyzer". An EDAX spectrum of complexes was computed on "Ametek EDAX with Apex software". To achieve IR and $^1$H-NMR spectra of the complexes "Perkin Elmer spectrum 400 spectrometer" and a Bruker Avance II 500 MHz NMR" spectrometer is employed respectively. UV–visible

absorption and diffused reflectance spectra are executed on "Shimadzu UV-3600 plus" using DMSO solution. For analyzing the thermal stability "Hitachi STA 7300 thermal analyzer" is employed with nitrogen atmosphere at a heating rate of 20 $^0$C from 40–900 $^0$C. SEM micrographs are performed on "Jeol JSM-6510 scanning electron microscope". The luminescence dynamics are analyzed from "Hitachi F-7000 fluorescence spectrophotometer" with a xenon lamp as excitation source with a slit width of 2.5 nm at 700 pmt voltages.

## Synthesis

Classically, solution precipitation method is employed for synthesis which involves precipitation of desired material from a mixture containing ethanolic solution of ligand (MPFA) (3 mmol) and Eu $(NO_3)_3$ (1 mmol) in water. A neutralization point is attained by the slow addition of NaOH (0.05) in the solution. This mixture is continuously stirred for 6 h and a white colored powder is collected for C1 binary complex [Eu(MPFA)$_3$.$H_2O$]. In a similar attempt, ternary complexes C2-C5 are prepared in conjunction with ethanolic solution of neo, bipy, batho and phen (1 mmol) [24]. To calculate the triplet state of ligand [Gd(L)$_3$.$2H_2O$] complex is synthesized in same manner. The synthetic route consisting of all the chemical structures of complexes C1-C5 is provided in Scheme 1.

Ligand (MPFA): IR(KBr): cm$^{-1}$ 3494 (b), 3014 (m), 1673 (w), 1491 (s), 1326 (m), 1169 (m), 1020 (m), 929 (w), 804 (w), 556 (s). H-NMR (DMSO), 500 MHz): 9.38 (s, -COOH), 7.6 (d, -CH, Ar–H), 7.3 (d, -CH, furan), 7.25 (t, -CH, Ar–H), 6.72 (d, -CH, furan), 2.38 (s, -$CH_3$).

Eu(MPFA)$_3$.$2H_2O$ (C1): White powder, yield 72%; IR(KBr): cm$^{-1}$ 3420 (b), 3022 (m), 2369(s), 1665 (s), 1483 (s), 1417 (m), 1318 (s), 1260 (m), 1161 (s), 1020 (m), 953 (w), 912 (m), 788 (m), 656 (m), 556(s), 507 (m), 491 (w). H-NMR (DMSO), 500 MHz): 7.7340 (d, 2H, Ar–H), 7.3157 (s, 2H, Ar–H), 6.7723 (s, 2H, furan), 2.43 (s, 3H, -$CH_3$).

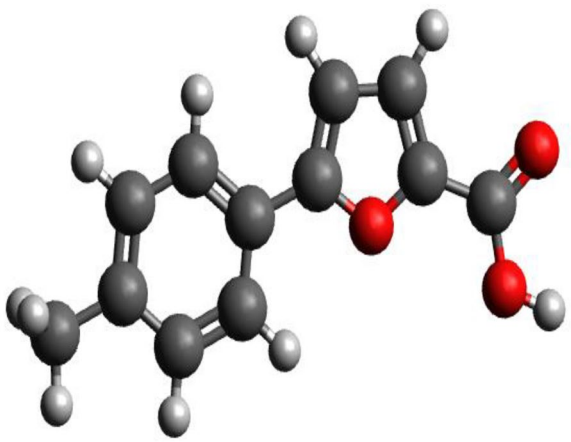

**Optimized structure of Ligand (MPFA)**

Optimized structure of Ligand (MPFA)

Eu(MPFA)$_3$.neo (C2): White powder, yield 71%; IR(KBr): cm$^{-1}$ 3428 (b), 3022 (m), 2916 (m), 2856 (w), 2352 (s), 1646 (w), 1496 (s), 1398 (w), 1275 (s), 1187 (m), 1107 (m), 1009 (s), 966 (m), 921 (s), 824 (m), 780 (m), 700 (m), 638 9w), 584 (w), 491 (s). H-NMR (DMSO), 500 MHz): 7.87 (m, 6H, Ar–H), 7.7340 (d, 4H, Ar–H), 7.3157 (s, 2H Ar–H), 6.7723 (s, 2H, furan), 2.43 (s, 3H, -$CH_3$).

Eu(MPFA)$_3$.bipy (C3): White powder, yield 71%; IR(KBr): cm$^{-1}$ 3420 (s), 3022 (s), 2916 (s), 2856 (s), 2355 (s), 1645 (w), 1520 (s), 1496 (s), 1398 (s), 1277 (m), 1187 (m), 1010 (s), 965 (m), 824 (w), 780 (m), 703 (m), 638 (w), 585 (w), 489 (s). H-NMR (DMSO), 500 MHz): 8.2649(s, 2H Ar–H), 7.9243(d, 2H, Ar–H), 7.09(m, 4H, Ar–H), 7.57 (m, 12H, Ar–H), 6.4210 (d, 1H, furan), 5.5076(d, 1H, furan),), 2.41 (s, 3H, -$CH_3$).

Eu(MPFA)$_3$.batho (C4): White powder, yield 73%; IR(KBr): cm-$^1$ 3022 (s), 2916 (s), 2856 (s), 2355 (s), 1645 (w), 1520 (s), 1496 (s), 1398 (s), 1277 (m), 1187 (m), 1010 (s), 965 (m), 824 (w), 780 (m), 703 (m), 638 (w), 585 (w), 489 (s). H-NMR (DMSO), 500 MHz): 8.6902(m, 12H, Ar–H), 7.9512 (d, 2H, Ar–H), 6.452(d, 1H, furan), 5.9289(d, 1H, furan), 2.46 (s, 3H, -$CH_3$).

Eu(MPFA)$_3$.phen (C5): White powder, yield 78%; IR(KBr): cm$^{-1}$ 3428 (b), 3022 (m), 2916 (m), 2856 (w), 2352 (s), 1646 (w), 1496 (s), 1398 (w), 1275 (s), 1187 (m), 1107 (m), 1009 (s), 966 (m), 921 (s), 824 (m), 780 (m), 700 (m), 638 9w), 584 (w), 491 (s). H-NMR (DMSO), 500 MHz): 8.3648(m, 4H, Ar–H), 7.65 (d, 2H, Ar–H), 7.36 (m, 12H, Ar–H), 6.4213(s, 1H, furan), 5.9419(s, 1H, furan), 2.42 (s, 3H, -$CH_3$).Scheme 1.Scheme showing chemical structures and process of synthesis of Eu(III) complexes C1-C.

## Result and Discussion

### Composition of the Complexes

The EDAX spectra provided faithful information about all the elements present in the complexes. The spectral peaks and EDAX mapping in Fig. 1a, b show the qualitative and quantitative composition of constituent elements (Eu, C, N, and O) present in the synthesized complexes respectively. Thus, the recorded results of EDAX are found in good correlation with the proposed chemical formulae of the synthesized complexes. The amount (%) of elements like Carbon, Hydrogen, Nitrogen and Europium ion present in the complexes is provided in Table 1.

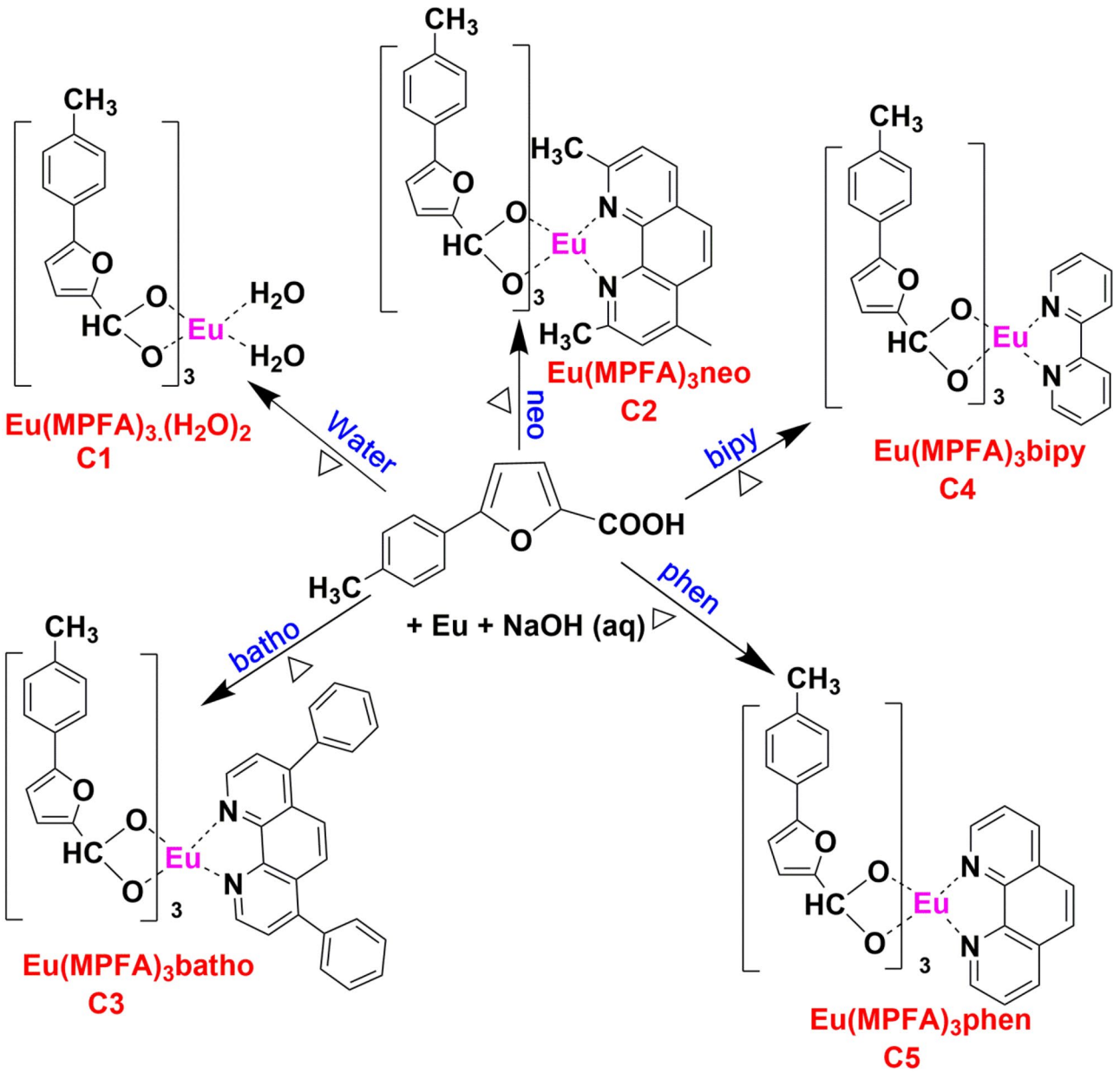


**Scheme 1** Scheme showing chemical structures and process of synthesis of Eu(III) complexes C1-C5

## FT-IR Spectra

The FT-IR spectral analyses are measured for ligand MPFA and its respective europium complexes C1-C5. The infrared spectra were executed in the range of 400–4000 $cm^{-1}$**.** The IR spectrum of free ligand (MPFA) displays two characteristic bands due to O–H stretching vibration of acidic group and ring modes of benzene ring at 3480 $cm^{-1}$ and 1681 $cm^{-1}$ respectively**.** The broad band owing to O–H in the free ligand observed at 3480 $cm^{-1}$ has been disappeared in the IR spectra of complexes C1-C5 [25, 26]. It confirms coordination of acidic oxygen to europium ion. All the complexes show strong peaks between 1560 and 1691 $cm^{-1}$ which can be assigned to stretching modes of C = C and C = O double bonds. In addition to this, a strong band due to C-H asymmetric vibrations is observed at 3288–3380 $cm^{-1}$ in the complexes. In the ternary complexes C2-C5 a strong band is observed in the range of 1495–1510 $cm^{-1}$ assigned to C = N stretching vibrations and at 556–598 $cm^{-1}$ due to Eu-N bonds (Table 2). These are strong evidences which declared that ligand MPFA has successfully coordinated to europium ion in the complexes. The spectral shapes in the IR spectra of all complexes C1-C5 are analogous with the ligand MPFA as shown in Fig. 2.

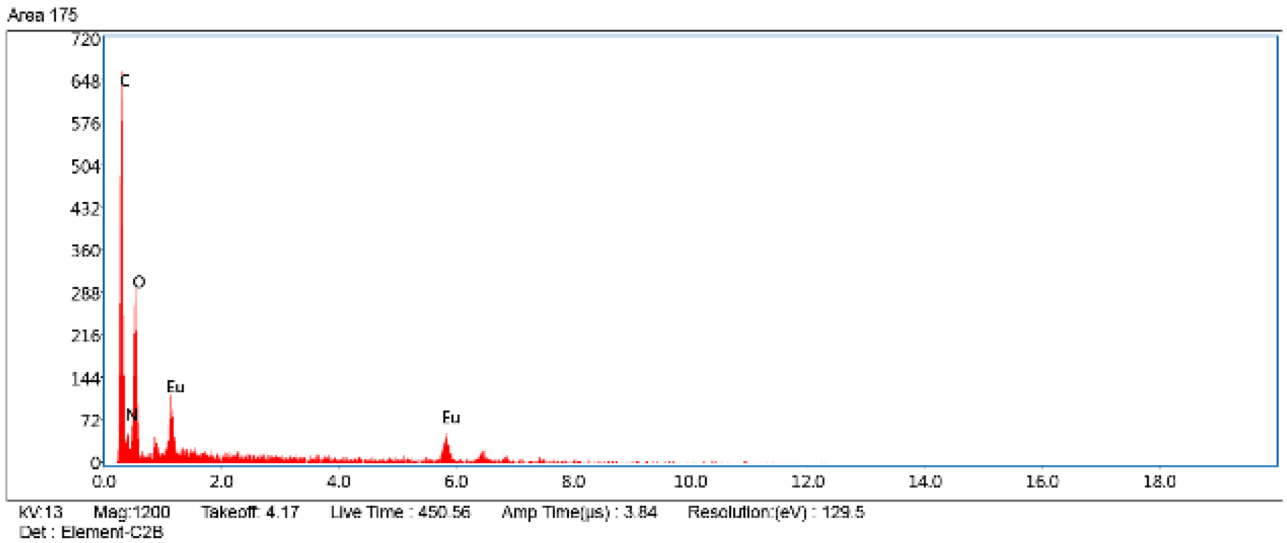


**(a)** EDAX spectral profile of complex [Eu $(MPFA)_3(Phen)$] (C5).

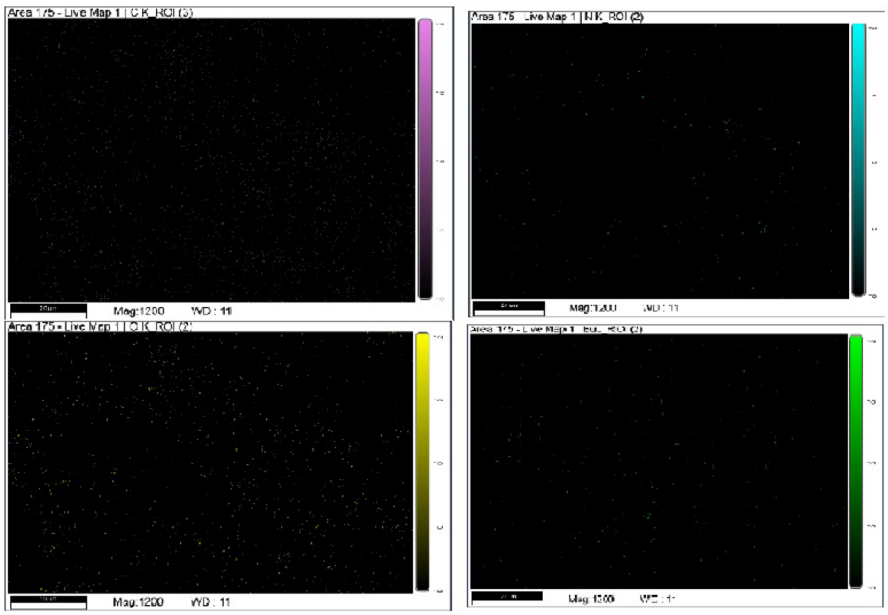

**(b)** EDAX mapping complex [Eu $(MPFA)_3(Phen)$] (C5).

**Fig. 1** **(a)** EDAX spectral profile of complex [Eu $(MPFA)_3(Phen)$] (C5) **(b)** EDAX mapping complex [Eu $(MPFA)_3(Phen)$] (C5)

**Table 1** Elemental compositions of ligand MPFA and its complexes C1-C5 in term of weight %

| Compound | Carbon | Hydrogen | Nitrogen | Europium |
|---|---|---|---|---|
| MPFA | 62.39 | 5.64 | - | - |
| C1 | 38.52 | 3.77 | - | 40.61 |
| C2 | 55.52 | 3.94 | 4.08 | 27.02 |
| C3 | 62.98 | 3.82 | 4.08 | 22.13 |
| C4 | 51.78 | 3.56 | 5.49 | 29.78 |
| C5 | 53.94 | 3.40 | 5.24 | 28.44 |

## H-NMR Characterization

$^1$H-NMR spectral description for ligand MPFA and complex C5 as a depictive of all the europium complexes were nicely illustrated in Fig. 3a, b. A marked difference between the proton magnetic resonance spectrum of uncoordinated ligand and europium complexes is the absence of a distinct (–OH) acidic proton of the carboxylate group peak at 9.38 ppm. In addition to this, the spectral profiles of bare ligand exhibit a singlet at 2.38 ppm due to methyl protons

**Table 2** Informative IR frequencies ($cm^{-1}$) of free MPFA ligand and Eu(III) Complexes (C1-C5)

| Compound | $\nu_{O-H}$ | $\nu_{C=O}$ | $\nu_{C=O}$ | $\nu_{C=N}$ | $\nu_{Eu-N}$ | $\nu_{Eu-O}$ |
|---|---|---|---|---|---|---|
| MPFA | - | 1725 (s) | 1590 (s) | - | - | - |
| C1 | 3280 (s, b) | - | 1590 (s) | - | - | 500 (s) |
| C2 | - | - | 1590 (s) | 1520(s) | 570 (m) | 497 (s) |
| C3 | - | - | 1591 (s) | 1525 (s) | 569 (s) | 489 (s) |
| C4 | 3406 (w, b) | - | 1592 (s) | 1535 (s) | 565 (s) | 495(s) |
| C5 | 3394 (w, b) | - | 1591 (s) | 1528 (s) | 575 (m) | 499 (s) |

w-weak, m-medium, s-strong, b-broad

($-CH_3$), doublet at 7.25 and 7.70 ppm due to protons (–CH) of benzene ring and two signals at 7.39 and 7.69 ppm due to protons (–CH) of furan ring. In the NMR spectra of complexes C1-C5 the signals related to aryl and furan protons exhibit downfield shift, evidenced the successful coordination of the europium ion with the acidic group of the ligand [27]. Evidently, the presence of additional signals in the resonance absorption spectra of europium complexes C2-C5 in the range of 7.0–8.0 ppm assigned the successful insertion of ancillary ligands in the coordination framework. Furthermore due to the paramagnetic behavior of Eu (III), all the resonance peaks in the complexes get broadened as compared to the ligand MPFA.

## Surface Morphology Analysis

One more relevant approach SEM is also employed to investigate the surface and morphological features of the europium complexes. The SEM micrographs of the complexes highlight the uniform distribution of the particles with the spherical shape. The best red-emitting C5 complex is shortlisted to represent the SEM image as a representative of all (Fig. 4). From the SEM images, it is evident that the particles are homogenous in nature in terms of their size and distribution.

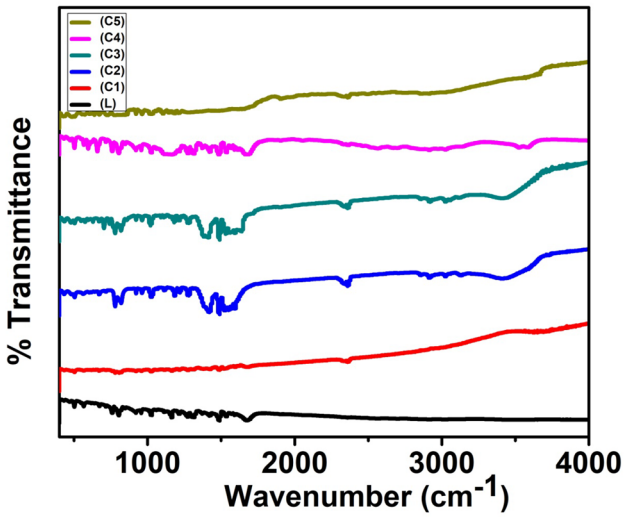


**Fig. 2** FT-IR spectra of ligand MPFA and all the Eu(III) complexes C1-C5

## Thermal Gravimetric Analysis (TGA)

Thermogravimetric analysis are carried out for the Eu(III) complexes C1-C5 within a temperature range of ambient temperature (40 $^0$C) to 900 $^0$C at a heating rate of 20$^0$ per minute under nitrogen flow. All the complexes show thermal stability up to 258 $^0$C and their decomposition started at this temperature. The thermal decomposition curve of all the complexes is almost alike, so the thermogram of complex C5 [$Eu(MPFA)_3Phen$] is depicted in Fig. 5 treated as representative of all (C1-C5) complexes. The decomposition event is driven in single step which involves the elimination of moisture, one ancillary ligand (phen) and three molecules of coordinated ligand MPFA up to the temperature range of 258-477 $^0$C. A horizontal line beyond 477 $^0$C suggests the presence of residual europium (III) oxide [28]. The thermal stability of the complexes up to 258 $^0$C demonstrated that these complexes can perform quite well as a suitable luminescent material for the fabrication of display devices.

## Electronic Spectroscopy

### UV–Visible Spectroscopy

Similar UV- visible spectral features are observed for the Eu(III) complexes as for the ligand which established that the $\pi$- $\pi^*$ energy states remains unaffected by the coordination sphere of the europium ion as ligand plays a major role in harvesting UV-light. The maximum absorption of ligand MPFA is situated at 302 nm (Fig. 6) while the complexes show their absorption maxima in the wavelength range of 300–303 nm owing to the perturbation induced by the europium ion in the coordination framework. In comparison to the uncoordinated ligand, enhanced absorption intensity is observed for complexes due to effective energy transfer as the energy difference between valence and conduction bands decreased in the complexes. Apart from binary, the absorption intensity of ternary complexes is also increased

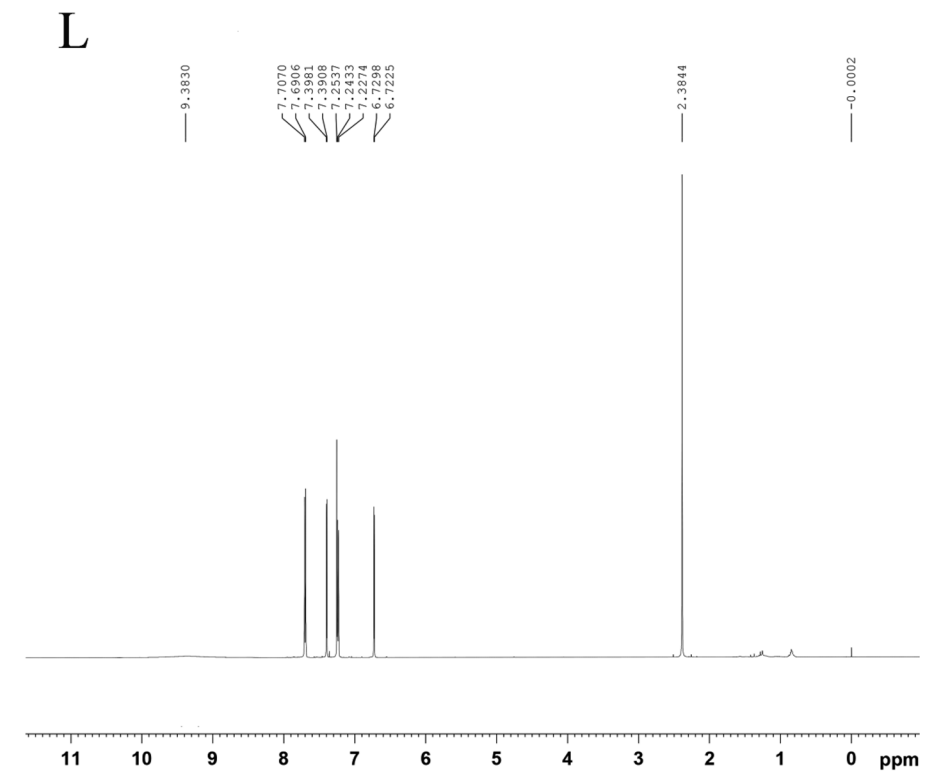


**(a)** $^{1}$H-NMR spectral profile of free ligand MPFA

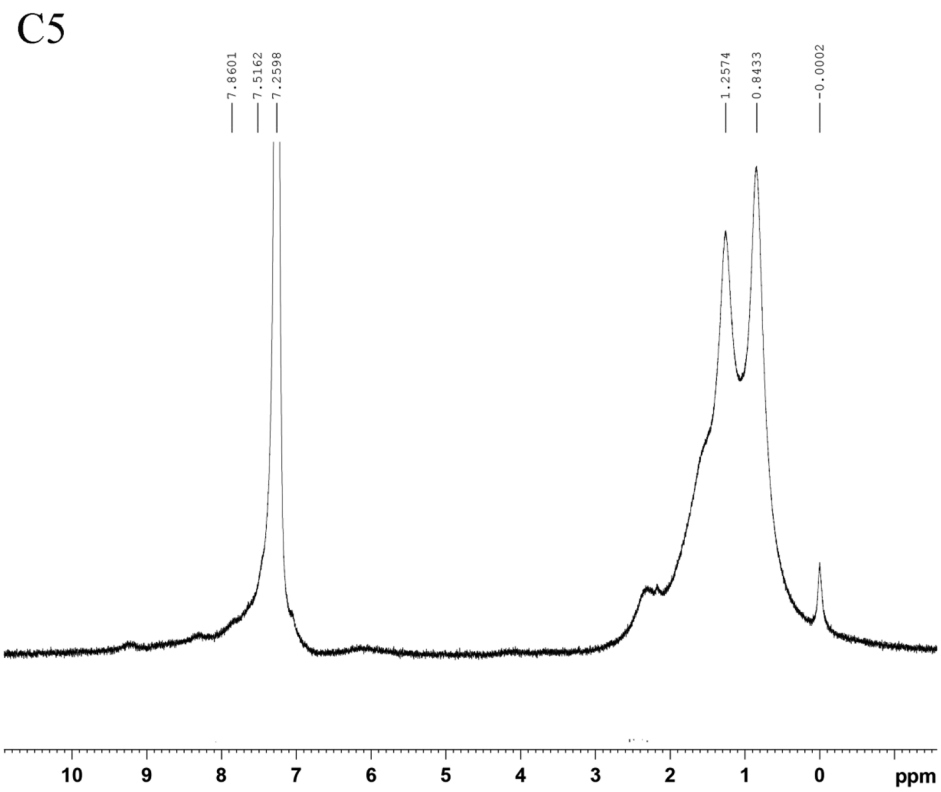


**(b)**.$^{1}$H-NMR spectra of complex [Eu(MPFA)$_3$.phen] (C5)

**Fig. 3** **(a)** $^{1}$H-NMR spectral profile of free ligand MPFA **(b)**.$^{1}$H-NMR spectra of complex [Eu(MPFA)$_3$.phen] (C5)

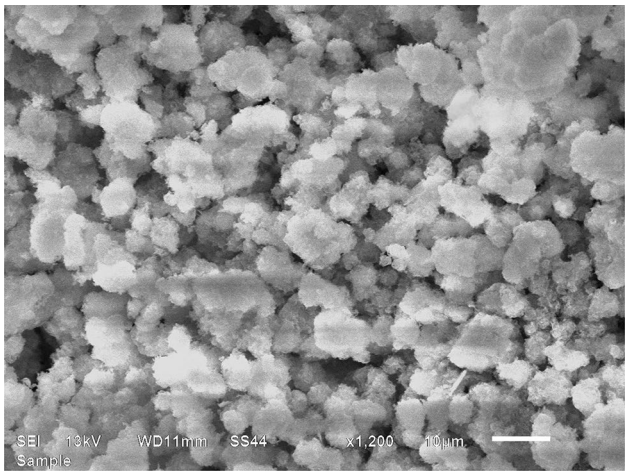


**Fig. 4** SEM image of complex [Eu(MPFA)$_3$(Phen)] (C5)

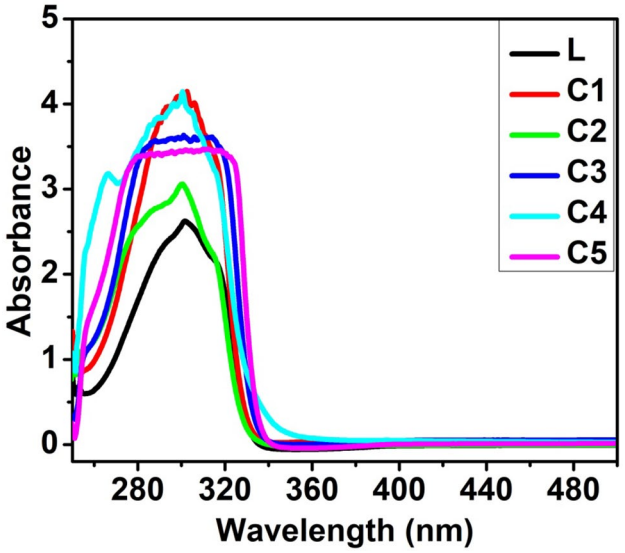


**Fig. 6** UV–visible absorption spectra of ligand MPFA and complexes C1-C5 in DMSO solution

suggesting that the ancillary ligands are successfully incorporated in the inner coordination sphere.

### Optical band gap analysis

The diffused reflectance spectral analysis of ligand MPFA and its respective europium complexes is determined at room temperature within the wavelength range of 200–800 nm in solid state. The optical energy band-gap ($E_g$) of ligand and complexes (C1-C5) is calculated by using diffused reflectance data via Kubelka–Munk function as represented by following equation:

$$F(R_\infty) = \frac{(1-R_\infty)^2}{2R_\infty} = \frac{K}{S} \tag{1}$$

In above expression, K and S refers to absorption and scattering coefficients while $F(R_\infty)$ symbolize their ratio.

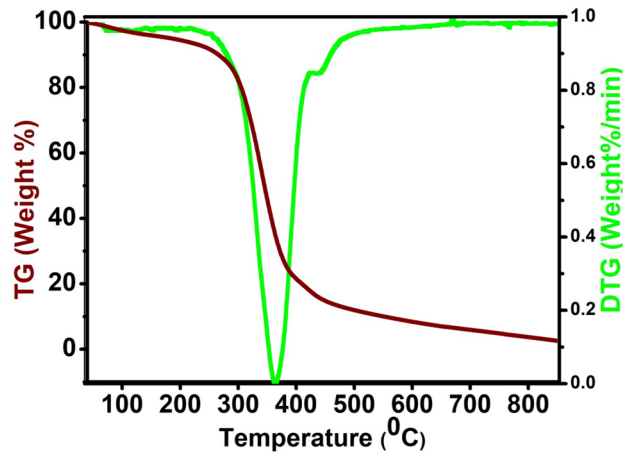


**Fig. 5** TGA/DTG thermogram of complex [Eu(MPFA)$_3$(Phen)] (C5)

By employing Wood-Tauc relation, Eg values are calculated according to the given equation:

$$[F(R_\infty)h\nu]^n = C(h\nu - E_g) \tag{2}$$

where $h\nu$ represents the energy of incident photons, C refers to the constant of proportionality. The Eg values are computed by extrapolation of tangent line on x-axis ($h\nu$) to zero in Tauc plots. The optical energy gap value for ligand MPFA is found to be more (3.58 eV) than its corresponding complexes (3.17–3.51) as shown in Table 3, designating that these complexes possess higher conductivity than ligand MPFA [29]. Notably, the Eg value for both the ligand MPFA and complexes are lying in the WBGs range (2-4 eV). Hence, it is fair to say that these complexes are potential contenders for optical applications in various fields such as luminescence thermometry, display devices and biological labeling [30]. Investigated Eg values are analogous for all the complexes hence Tauc plot of complex C5 is selected as a representative of all complexes. Figure 7a, b represents the Tauc plot of ligand MPFA and Complex C5 and their diffused reflectance spectra is given in insets. In addition to this, band gap values can be used for the estimation of refractive index (n) of europium complexes (C1-C5) in the given expression:

$$\frac{n^2-1}{n^2+1} = 1 - \sqrt{\frac{E_g}{20}} \tag{3}$$

The calculated values of refractive index for ligand MPFA and complexes are indexed in Table 4. The refractive indexes of ligand MPFA and complexes are found comparable with

**Table 3** Optical band gap value ($E_g$), luminescence lifetime (τ), radiative rate constant ($A_{rad}$), quantum efficiency and Judd–Ofelt parameters $\Omega_\lambda$ of C1-C5 complexes

| Complexes | $E_g$ (eV) | τ (ms) | $A_{rad}$ ($S^{-1}$) | η(%) | $A_{tot}$($S^{-1}$) | $\Omega_2$, ($10^{-20}cm^2$) |
|---|---|---|---|---|---|---|
| C1 | 3.50 | 0.186 | 224.18 | 8.18 | 2513.13 | 3.33 |
| C2 | 3.44 | 0.588 | 225.20 | 13.3 | 1462.32 | 3.38 |
| C3 | 3.51 | 0.739 | 236.43 | 17.3 | 1128.82 | 3.50 |
| C4 | 3.17 | 0.832 | 238.25 | 19.9 | 954,54 | 3.74 |
| C5 | 3.40 | 0.991 | 243.03 | 24.1 | 765.97 | 3.56 |

that of metal oxide like zirconium oxide (n = 2.10) and zinc oxide (n = 2.00), hence these luminescent complexes seem to be promising for further developments in designing of lighting devices [31].

## Photoluminescence Spectroscopy

Luminescence is an extremely responsive analytical technique able to sense minute differences. In order to get best luminescence, efforts have essentially been focused on recording excitation spectra of the europium complexes. The excitation spectral studies of the complexes are scanned in solid state in the spectral range of 200–500 nm by fixing the emission wavelength at 618 nm. From the Fig. 8 it is evident that the relative intensities of the transitions are different while the spectral shape looks alike which suggest the homogenous nature of chemical environment around the europium ion [32]. The excitation maximum peak in the complexes is located at 353 nm. Excitation spectra of complexes reflect a broad band within 300–450 nm which can be considered as a product of electronic transitions takes place in ligand MPFA. A spectral line of less intensity is also observed in the spectral region of 471 nm. All these findings proved to be helpful in concluding that direct excitation of f-f transitions in Eu(III) ion seems to be unfavorable but fortunately the ligand MPFA proved to be efficient antenna for sensitizing the Eu(III) ion.

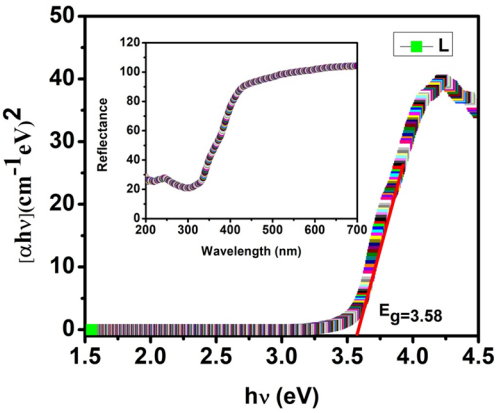


**(a)** Tauc plot of ligand MPFA whereas its inset shows the resultant DR spectra.

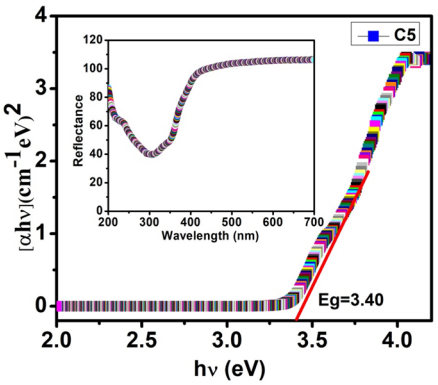


**(b)**. Tauc plot of Eu(III) complex [Eu(MPFA)$_3$phen] (C5) whereas its inset shows the resultant DR spectra.

**Fig. 7** **(a)** Tauc plot of ligand MPFA whereas its inset shows the resultant DR spectra **(b)**. Tauc plot of Eu(III) complex [Eu(MPFA)$_3$phen] (C5) whereas its inset shows the resultant DR spectra

The photo-emission spectra of complexes are obtained in solid state at room temperature within the wavelength range of 400–700 nm by monitoring the luminescence intensity as a function of emission wavelength. Upon photo-excitation, the excitation energy transfer from the blue luminescent chromophoric ligand to europium ion produced strong and spiky metal centered red colored emission. The emission spectra comprises of three well-identified, sharp spectral peaks with sufficient resolution in the expected spectral range at 582, 595 and 615 nm attributed to the electronic transitions from $^5D_0 \rightarrow {}^7F_J$ states (J = 0–4) (Fig. 9). The emission peak at 582 nm refers to $^5D_0 \rightarrow {}^7F_0$ transition having low intensity as it is forbidden in both magnetic and electric field. A sharp band with high intensity at 595 nm symbolizes $^5D_0 \rightarrow {}^7F_1$ transition used to calibrate the photoemission spectra as its luminescence is independent of chemical environment [33]. A highly intense peak situated at 615 nm due to $^5D_0 \rightarrow {}^7F_2$ electric dipole transition dominates the luminescence dynamics and responsible for the red colored emission. This transition is greatly affected by the polarizable ligand field conveys the presence of unsymmetrical ligand field around the europium ion and hence the luminescence intensity also gets affected accordingly [34, 35]. It is noteworthy to mention that ligand assisted residual emission is not observed in 400–480 nm spectral range which signifies the efficient transfer of photons absorbed by the ligand MPFA to the excites state (4f) of the Eu(III) ion. The

**Table 4** The chromaticity coordinates, correlated color temperatures (CCT), refractive index (n) and color purity (CP) of emission color emitted by europium complexes

| Complex | Color coordinates (x, y) | Color coordinates (u, v) | CCT(K) | n | CP (%) |
|---|---|---|---|---|---|
| C1 | 0.604, 0.394 | 0.252, 0.561 | 2811 | 2.27 | 67.03 |
| C2 | 0.574, 0.422 | 0.390, 0.541 | 1754 | 2.03 | 68.39 |
| C3 | 0.556, 0.440 | 0.396, 0.361 | 1826 | 2.01 | 64.24 |
| C4 | 0.536, 0.452 | 0.401, 0.539 | 1868 | 2.03 | 66.05 |
| C5 | 0.500, 0.402 | 0.447, 0.532 | 2640 | 2.00 | 63.43 |

luminescence intensity of complexes C2-C5 is considerably high as ancillary ligands give rise to perfect asymmetry in the inner coordination sphere of the complexes. These outstanding luminescent features of europium complexes make them proficient for their applications in field of light emitting devices.

Furthermore, branching ratio of these emission lines is evaluated from the ratio of integrated emission intensity of the respective transition to the total integrated emission intensity. The branching ratios of most intense $^5D_0 \rightarrow {}^7F_2$ transition are estimated more than 50% which boost their application in solid state lasers, as the working of laser depend on the high integrated emission intensity of spectral lines. The extent of distortion in the centre of symmetry around the europium ion is assessed from asymmetric ratio which is calculated by the intensity ratio of the $^5D_0 \rightarrow {}^7F_2$ to $^5D_0 \rightarrow {}^7F_1$ transition. From Table 5, it is justified that the values asymmetric ratio are consistent with the presence of distorted ligand field around europium ion.

In order to further investigate the optical features of the europium complexes, luminescence lifetime of resonating level of $^5D_0$ of Eu(III) ion is obtained from decay curves by monitoring the excitation and emission wavelength employing a well known exponential equation $I = I_0\exp(-t/\tau)$ and curve fitting program (Fig. 10). The luminescence decay profile of complexes follow monoexponential behavior of decay curve which is attributed to the presence of one kind of emitting species. Furthermore it is well documented that encapsulation of vibronic quenchers (water molecules) in the binary complexes by ancillary ligands, reinforces the luminous intensity of the ternary complexes. These complexes have been of great importance for photonic application in lasers and OLEDs owing to their lengthened luminescent lifetime.

### Judd–Ofelt analysis

According to the photoemission spectra, the radiative transition rates ($A_{rad}$) for each ($^5D_0$-$^7F_J$) transition can be calculated by selecting $^5D_0$- $^7F_1$ transition as a reference (50 $s^{-1}$) because this transition seems to be insensitive to the local field environment of the Eu(III) ion. The integrated area under the curve ($I_{0J}$) and the energy bery-centre ($\nu_{0J}$) obtained from the spectral data are fitted into the following expression to determine $A_{0J}$ related to distinct transitions ($^5D_0$-$^7F_J$) (J = 0, 1, 2, 3).

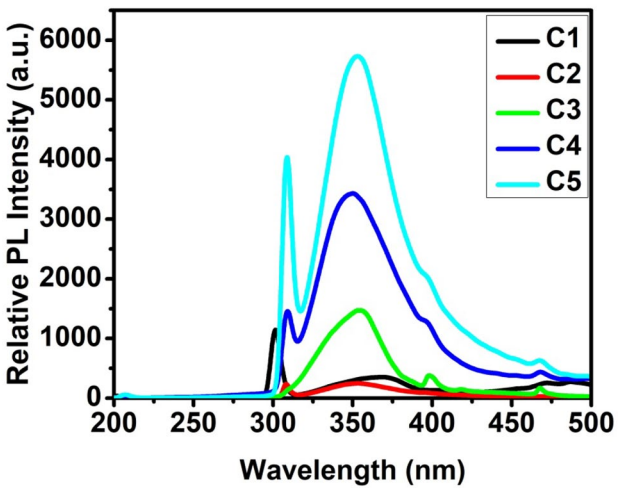


**Fig. 8** Solid state excitation spectral profile of complexes C1-C5 executed at 618 nm

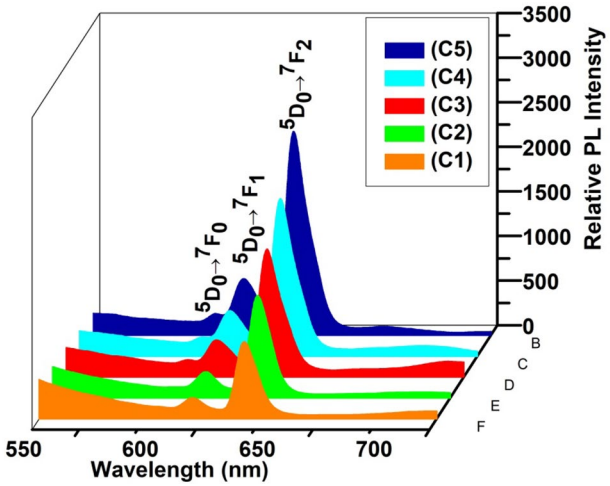


**Fig. 9** Photoluminescence emission spectra of complexes C1-C5 in the solid state at room temperature excited at 353 nm

**Table 5** Branching (β) and asymmetric ratios (r) of every $^5D_0 \rightarrow {}^7F_J$ transition of Eu (III) complexes

| Complex | $^5D_0 \rightarrow {}^7F_0$ | $^5D_0 \rightarrow {}^7F_1$ | $^5D_0 \rightarrow {}^7F_2$ | $r = I_2/I_1$ |
|---|---|---|---|---|
| C1 | 10.68 | 22.66 | 66.65 | 2.94 |
| C2 | 6.96 | 21.59 | 71.40 | 3.30 |
| C3 | 5.70 | 22.78 | 71.50 | 3.13 |
| C4 | 12.14 | 32.74 | 75.12 | 3.45 |
| C5 | 14.33 | 20.97 | 78.34 | 4.22 |

$$A_{0J} = A_{01}(I_{0J}/I_{01})(\nu_{01}/\nu_{0J}) \quad (4)$$

Total radiative rates ($A_{rad}$) of the complexes can be computed by summing over the radiative rates related to the ($^5D_0$-$^7F_J$) transitions of Eu(III) ion [36, 37]. The radiative and non-radiative processes not only depopulate the $^5D_0$ state but luminescence lifetime is also getting influenced according to the equation given below:

$$A_{Total} = 1/\tau = A_{rad} + A_{nrad} \quad (5)$$

The luminescence quantum efficiency for the resonating levels can be evaluated which communicates how well the radiative processes compete with the non-radiative processes. Internal quantum efficiency measures the radiative relaxation of $^5D_0$ state.

$$\eta = A_{rad}/A_{rad} + A_{nrad} \quad (6)$$

From Table 3, ternary complexes exhibited higher luminescence quantum efficiency which corroborates with the PL emission results. The results showed that the incorporation of ancillary ligand enhances the quantum efficiency via synergistic effect.

The Judd–Ofelt theory is functional implementation for predicting the inner shell 4f-4f electronic transitions. The Judd–Ofelt intensity parameters $\Omega_\lambda$ ($\lambda = 2$) can be accessed from PL emission spectra by employing following equation:

$$\Omega_\lambda = \frac{3.h.A_{0J}}{64.\pi^4 e^2 \bar{v}^3 \chi < {}_0{}^5D|U^\lambda|_J{}^7F >^2} \quad (7)$$

**Table 6** Excitation energy parameters of main ligand MPFA and ancillary ligands (batho, bipy and phen) in $cm^{-1}$ corresponding to excited energy level of $Eu^{3+}$ ion

| Ligands | $E(S_1)$ | $E(T_1)$ | $\Delta E(S_1\text{-}T_1)$ | $\Delta E_0(T_1—{}^5D_1)$ | $\Delta E_0(T_1—{}^5D_0)$ |
|---|---|---|---|---|---|
| MPFA | 29,411 | 22,779 | 6632 | 4088 | 5529 |
| batho | 29,000 | 21,000 | 8000 | 2309 | 3759 |
| bipy | 29,900 | 22,900 | 7000 | 4209 | 5659 |
| phen | 31,000 | 22,100 | 8900 | 3409 | 4859 |

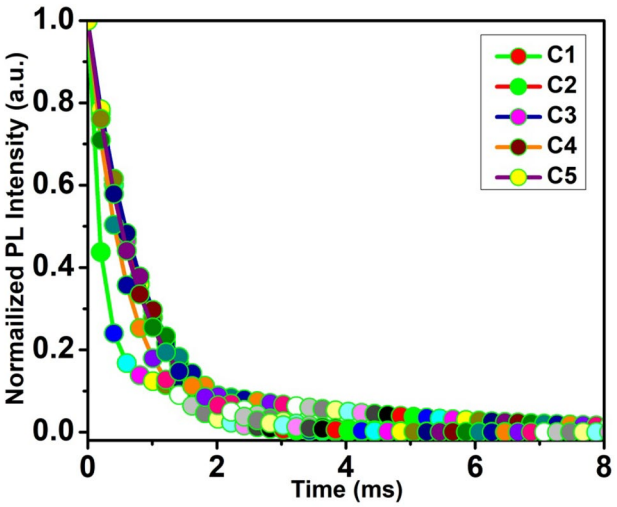


**Fig. 10** The decay curves for the luminescence of Eu(III) ion in complexes C1-C5

where, the squared reduced matrix elements are $\langle 5Do|U^{(\lambda)}|7_{F2}\rangle^2 = 0.0032$, $h$ refers to Planck's constant and $\chi$ symbolize the Lorentz local field correction term and is known by $n(n^2+2)^2/9$, the value of n is taken as 1.5. The higher values of Judd–Ofelt parameter ($\Omega_2$) in the results of complexes (C2-C5) demonstrated that ancillary ligands improved the luminescence properties of Eu(III) ion by introducing asymmetry in the coordination sphere [38]. The predicted radiative rates ($A_{rad}$), non-radiative ($A_{nrad}$) and the internal quantum efficiency (η) are presented in Table 3.

## Color purity

To better understand the extent of saturation of a particular color emitted by europium complexes the color purity is checked by the employing CIE color coordinates which are extracted from photoemission data in MATLAB software (Fig. 11a). The quantitative estimation of color purity is accomplished by taking illumination source ($x_i = 0.333$, $y_i = 0.333$) as standard as per given expression:

$$CP = \left[\frac{(x-x_i)^2 + (y-y_i)^2}{(x_d-x_i)^2 + (y_d-y_i)^2}\right]^{\frac{1}{2}} \quad (8)$$

The dominant coordinates ($x_d$, $y_d$) in the above expression are predicted by drawing a line through illumination coordinates ($x_i$, $y_i$) of respective europium complexes. The color purity of ternary complexes is noted with high values as reported in Table 4, strengthened the opinion that ancillary ligands boost the beneficial characteristics of observed

photoluminescence. Thus, these red light emitting europium complexes with high color purity confirms their applicability in the lighting and display devices.

The following expression is used to calculate the correlated color temperatures (CCT) of the europium complexes:

$$CCT = 449t^3 + 3525t^2 + 6823.3t + 5520.33 \quad (9)$$

Here, t refers to the ratio of $(x - x_e)$ to $(y_e - y)$ where $x_e$ = 0.3320, $y_e$ =0.1854. The calculated values of CCT for synthesized complexes are found in the range of 1754–2811 and lies at lower temperatures as according to the black body radiation theory. CIE color coordinates (x, y) 1931 are used to predict CIE color space (u, v) 1960 as per given equation:

$$u = \frac{4x}{-2x + 12 + 3} \quad (10)$$

$$v = \frac{6y}{-2x + 12 + 3} \quad (11)$$

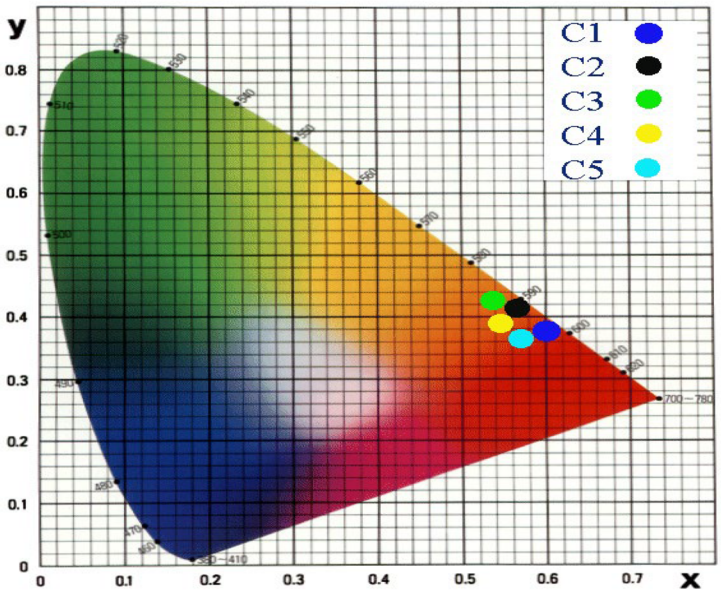


**(a)** Chromaticity diagram showing color coordinate (x, y) of Eu(III) complexes C1-C5.

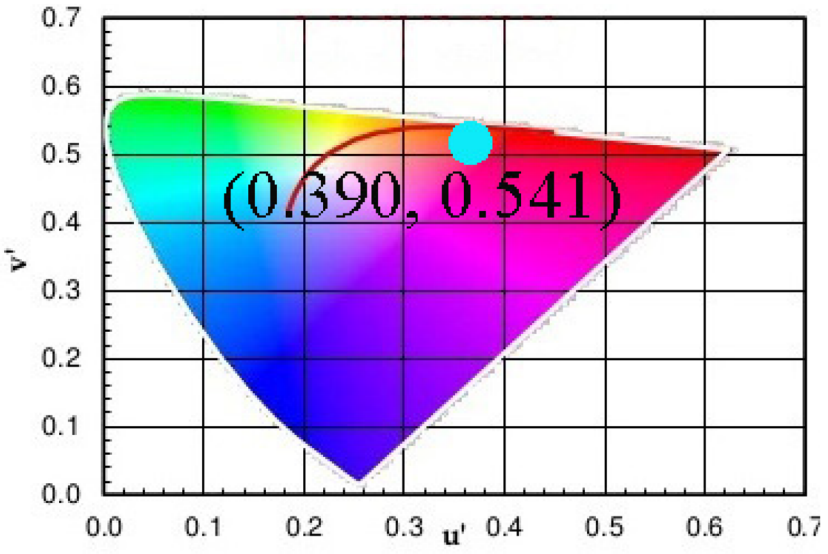


**(b)** The color coordinates (u, v) of Eu(III) complexes C1-C5.

**Fig. 11** **(a)** Chromaticity diagram showing color coordinate (x, y) of Eu(III) complexes C1-C5 **(b)** The color coordinates (u, v) of Eu(III) complexes C1-C5

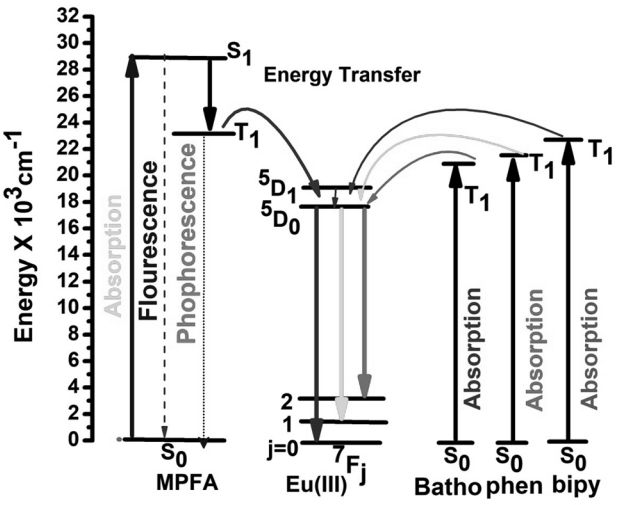


**Fig. 12** Schematic energy level diagram showing intramolecular energy transfer process of Eu (III) complexes

The color coordinates (u, v) of the europium complexes are in accordance with the CCT values (Fig. 11b). The color coordinates (u, v) and the CCT values of the synthesized complexes is given in Table 4. Based on the CCT values, these complexes proved to be better luminescent materials with technological potential.

### Energy Transfer Pathway

In order to gain ground in sensing the sensitization pathway, energy transfer pathway is deeply studied. This energy transfer phenomenon can be assigned to direct excitation of ligand MPFA from singlet ($S_0$) ground state to the singlet ($S_n$) excited state. These excited states ($S_n$) drift down to very short lived ($S_1$) lowest excited singlet state and ($T_1$) excited triplet state facilitated by radiative internal conversion (IC) and non-radiative intersystem crossing (ISC) respectively. Now the excitation energy of triplet state is dissipated to the resonating levels of europium ions $^5D_J$ (J = 0, 1, 2, 3), followed by subsequent emission to the $^5D_0$ level [39–42]. In this way, Eu(III) ion show red colored emission in the visible range owing to transitions that occurs in different electronic levels. It is well known that the efficiency of energy transfer depends on the perfect matching of lowest triplet state and the resonating levels of europium ion [43]. In this concern, the position of triplet energy state had been determined by measuring the phosphorescence spectra of gadolinium(III) ion complex with the ligand and singlet energy state had been calculated by referring UV–visible spectra of ligand MPFA. The required energy gap between singlet (29,411 $cm^{-1}$, 340 nm) and triplet energy states (22,779 $cm^{-1}$, 439 nm) had been found in the optimal range (≥ 5000 $cm^{-1}$) as suggested by Reinhoudt's empirical rule. According to Latva, it is necessary that the energy gap of triplet state and resonating level of Eu(III) ion must come between 2500–5000 $cm^{-1}$(Latva defined range). As shown in Table 6, all the required criteria of eligibility for a "perfect antenna" had been fulfilled by the ligand MPFA and hence proved an effective sensitizer for the Eu(III) ion). The observed trends in the luminescence intensity reveals sharp and intense emission in ternary complexes as the ancillary ligand enhances sensitization whereas due to nonradiative deactivation assisted by vibronic coupling with the ligand and the solvent molecule, binary complexes C1 give reduced luminescence. The triplet and singlet energy states of the ancillary ligands (bipy, batho, and phen) are in accordance with the reported literature. Table 6. In an effort to demonstrate all the related parameters of europium complexes, energy level diagram of C5 complex is displayed in Fig. 12.

## Conclusion

In summary, a new family of five europium complexes with furoic acid functionalized ligand had been synthesized through a tailor made solution precipitation approach. The spectroscopic and photophysical features had been investigated by the use of different analytical techniques. The findings of EDAX, FT-IR, NMR, UV–visible spectroscopy, elemental (CHN) assure the coordination of ligand binding sites with the europium ion. These Eu(III) complexes possess good thermal stability and excellent optoelectronic features as predicted from TGA and PL analysis. Diffuse reflectance spectral studies confirm their applications in the semiconductors. All the complexes show sharp red emission validated by CIE color coordinates, color purity, asymmetric ratio and CCT values. Our results may enrich the family of lanthanide metal organic complexes based on furoic acid ligands with a bright hope for the better future.

**Acknowledgements** This research work did not receive any funding assistance from funding agencies in public, commercial or not from profit sector.

**Author Contribution** All authors contributed to the study conception, data curation, software validation and design. Material preparation, data collection and analysis were performed by Manisha Bedi. The first draft of the manuscript was written by Manisha Bedi. Review-writing and editing was performed by V. B. Taxak, S.P. Khatkar. The work was supervised by Priti Boora Doon. All authors read and approved the final manuscript.

## Declarations

**Ethics approval** This is our original research work and it highlights new dimensions in the field of luminescent materials by utilizing various

advanced techniques. The work has not been published before; it is not under consideration for publication anywhere else; and publication has been approved by all co-authors and the responsible authorities at the institute where the work has been carried out. Moreover, the authors are ready to follow all norms of the publications like copy right etc.

**Consent to Participate** Informed consent was obtained from all individual participants included in the study.

**Consent for Publication** The authors affirm that human research participants provided informed consent for publication of all the images in Figures.

**Conflict of Concern** There are no conflicts of concern to declare.

## References


1. Francis B, Raj DBA, Reddy MLP (2010) Highly efficient luminescent hybrid materials covalently linking with europium (III) complexes via a novel fluorinated β-diketonate ligand: synthesis, characterization and photophysical properties. Dalt Trans 39:8084–8092
2. Biju S, Raj DBA, Reddy MLP, Kariuki BM (2006) Synthesis, crystal structure, and luminescent properties of novel Eu3+ heterocyclic β-diketonate complexes with bidentate nitrogen donors. Inorg Chem 45:10651–10660
3. Yan B, Zhang H, Wang S, Ni J (1998) Intramolecular energy transfer mechanism between ligands in ternary rare earth complexes with aromatic carboxylic acids and 1, 10-phenanthroline. J Photochem Photobiol A Chem 116:209–214
4. Ahmed Z, Iftikhar K (2012) Synthesis, luminescence and NMR studies of lanthanide (III) complexes with hexafluoroacetylacetone and phenanthroline. Part II, Inorganica Chim Acta 392:165–176
5. Raj DBA, Biju S, Reddy MLP (2008) One-, two-, and three-dimensional arrays of Eu3+-4, 4, 5, 5, 5-pentafluoro-1-(naphthalen-2-yl) pentane-1, 3-dione complexes: synthesis, crystal structure and photophysical properties. Inorg Chem 47:8091–8100
6. Binnemans K, Lenaerts P, Driesen K, Görller-Walrand C (2004) A luminescent tris (2-thenoyltrifluoroacetonato) europium (III) complex covalently linked to a 1, 10-phenanthroline-functionalised sol–gel glass. J Mater Chem 14:191–195
7. Irfanullah M, Iftikhar K (2010) New hetero-dilanthanide complexes containing Ln1 (fod) 3 and Ln2 (fod) 3 fragments (Ln= Pr–Nd; Nd–Sm; Eu–Tb and Ho–Er) linked by bis-diimine bridging ligand. Inorg Chem Commun 13:694–698
8. Irfanullah M, Iftikhar K (2009) New dinuclear lanthanide (III) complexes based on 6, 6, 7, 7, 8, 8, 8-heptafluoro-2, 2-dimethyl-3, 5-octanedione and 2, 2′-bipyrimidine. Inorg Chem Commun 12:296–299
9. Li X, Wang X-W, Zhang Y-H (2008) Blue photoluminescent 3D Zn (II) metal-organic framework constructing from pyridine-2, 4, 6-tricarboxylate. Inorg Chem Commun 11:832–834
10. Gao H-L, Hu C-C, Zhang H, Wang H-T, Yang A-H, Cui J-Z (2012) Three polymers based on pyridine-2, 3, 5, 6-tetracarboxylic acid: syntheses, crystal structures and luminescent properties. Inorg Chem Commun 23:9–13
11. Lunstroot K, Driesen K, Nockemann P, Van Hecke K, Van Meervelt L, Görller-Walrand C, Binnemans K, Bellayer S, Viau L, Le Bideau J (2009) Lanthanide-doped luminescent ionogels. Dalt Trans 298–306
12. da Rosa PPF, Kitagawa Y, Hasegawa Y (2020) Luminescent lanthanide complex with seven-coordination geometry. Coord Chem Rev 406:213153
13. Yue B, Chen Y-N, Chu H-B, Qu Y-R, Wang A-L, Zhao Y-L (2014) Synthesis, crystal structures and fluorescence properties of dinuclear Tb (III) and Sm (III) complexes with 2, 4, 6-tri (2-pyridyl)-1, 3, 5-triazine and halogenated benzoic acid. Inorganica Chim Acta 414:39–45
14. Annapurna K, Dwivedi RN, Kundu P, Buddhudu S (2003) Fluorescence properties of Sm3+: ZnCl2□ BaCl2□ LiCl glass. Mater Res Bull 38:429–436
15. Görller-Walrand C, Binnemans K (1998) Spectral intensities of ff transitions. Handb Phys Chem Rare Earths 25:101–264
16. Nakanotani H, Adachi C (2014) A new route of triplet harvesting for high-efficiency organic light-emitting diodes. 日本画像学会誌 53:509–516
17. Bala M, Kumar S, Devi R, Khatkar A, Taxak VB, Boora P, Khatkar SP (2018) Synthesis, photoluminescence behavior of green light emitting Tb (III) complexes and mechanistic investigation of energy transfer process. J Fluoresc 28:775–784
18. Khanagwal J, Kumar R, Hooda P, Khatkar SP, Taxak VB (2021) Designing of luminescent complexes of europium (III) ion with hydroxyl ketone and nitrogen donor secondary ligands for improving the luminescence performance and biological actions. Inorganica Chim Acta 525:120463
19. Divya V, Reddy MLP (2013) Visible-light excited red emitting luminescent nanocomposites derived from Eu3+-phenathrene-based fluorinated β-diketonate complexes and multi-walled carbon nanotubes. J Mater Chem C 1:160–170. https://doi.org/10.1039/C2TC00186A
20. Allendorf MD, Bauer CA, Bhakta RK, Houk RJT (2009) Luminescent metal–organic frameworks. Chem Soc Rev 38:1330–1352
21. Rabasovic MS, Sevic D, Krizan J, Terzic M, Mozina J, Marinkovic BP, Savic-Sevic S, Mitric M, Rabasovic MD, Romcevic N (2015) Characterization and luminescent properties of Eu3+ doped Gd2Zr2O7 nanopowders. J Alloys Compd 622:292–295
22. Zhou J, Chen Y, Xian S, Liang Y, Huang G, Wang L, Yang X (2021) Eu (III)-based metal-organic-frameworks luminescent probe and its sensing properties for nitrobenzene and Cu (II). J Solid State Chem 304:122542
23. Tanwar V, Singh S, Gupta I, Kumar P, Kumar H, Mari B, Singh D (2021) Preparation and luminescence characterization of Eu (III)-activated Forsterite for optoelectronic applications. J Mol Struct 131802
24. Dhankhar P, Devi R, Devi S, Chahar S, Dalal M, Taxak VB, Khatkar SP, Boora P (2019) Synthesis and photoluminescent performance of novel europium (III) carboxylates with heterocyclic ancillary ligands. Rare Met 1–11
25. Langyan R, Chauhan A, Lohra S, laj Dhania S (2020) Judd-Ofelt analysis of some novel Eu3+ complexes featuring Kojic acid and N, N'-donor ligands. J Photochem Photobiol A Chem 401:112752
26. Devi R, Vaidyanathan S (2020) Narrow band red emitting europium complexes and their application in smart white LEDs and vapoluminescent sensors. Dalt Trans 49:6205–6219
27. Lemmetyinen H, Vuorimaa E, Jutila A, Mukkala V, Takalo H, Kankare J (2000) A time-resolved study of the mechanism of the energy transfer from a ligand to the lanthanide (III) ion in solutions and solid films. Luminescence 15:341–350
28. Khanagwal J, Kumar R, Bedi M, Khatkar SP, Taxak VB (2021) Enhanced Optoelectronic and Biological Potential of Virescent-Glowing Terbium (III) Complexes with Pyrazole Acid. J Electron Mater 50:2656–2668
29. Khanagwal J, Khatkar SP, Dhankhar P, Bala M, Kumar R, Boora P, Taxak VB (2020) Synthesis and photoluminescence analysis of europium (III) complexes with pyrazole acid and nitrogen containing auxiliary ligands. Spectrosc Lett 53:625–647
30. Sun H-J, Fu X-T, Chu H-B, Du Y, Lin X-M, Li X, Zhao Y-L (2011) Synthesis, characterization and luminescence property of

ternary rare earth complexes with azatriphenylenes as highly efficient sensitizers. J Photochem Photobiol A Chem 219:243–249
31. Punia M, Khatkar SP, Taxak VB, Dhankhar P, Boora Doon P (2021) Synthesis of cool white light emitting novel dysprosium (Dy3+) complexes with tetradentate β-ketoamide and heterocyclic auxiliary ligands. Luminescence
32. Hooda P, Taxak VB, Malik RK, Punia M, Ahlawat P, Khatkar SP, Kumar R (2021) Designing of emerald terbium (III) ions with β-ketocarboxylic acid and heterocyclic ancillary ligands for biological and optoelectronic applications. Luminescence
33. Bhat SA, Iftikhar K (2020) Optical properties and intensity parameters of UV excited efficient red emitting europium complexes containing fluorinated 1, 3-dione as primary sensitizer in solution, solid and PMMA thin films. Opt Mater (Amst) 99:109600. https://doi.org/10.1016/j.optmat.2019.109600
34. Binnemans K (2005) Handbook on the physics and chemistry of rare earths. Elsevier, Amsterdam 35:107
35. Carnall WT, Fields PR, Rajnak K (1968) Electronic energy levels in the trivalent lanthanide aquo ions. I. Pr3+, Nd3+, Pm3+, Sm3+, Dy3+, Ho3+, Er3+, and Tm3+. J Chem Phys 49:4424–4442
36. Ofelt GS (1963) Structure of the f 6 Configuration with Application to Rare-Earth Ions. J Chem Phys 38:2171–2180
37. Judd BR (1962) Optical Absorption Intensities of Rare-Earth Ions. Phys Rev 127:750–761. https://doi.org/10.1103/PhysRev.127.750
38. Racah G (1949) Theory of complex spectra. IV Phys Rev 76:1352
39. Binnemans K (2015) Interpretation of europium(III) spectra. Coord Chem Rev 295:1–45. https://doi.org/10.1016/j.ccr.2015.02.015
40. T. Főrster (1959) 10th Spiers Memorial Lecture. Transfer mechanisms of electronic excitation, discuss. Faraday Soc 27:7–17. https://doi.org/10.1039/DF9592700007.
41. Dexter DL (1953) A theory of sensitized luminescence in solids. J Chem Phys 21:836–850
42. Latva M, Takalo H, Mukkala V-M, Kankare J (1998) Evaluation of solution structures of highly luminescent europium (III) chelates by using laser induced excitation of the 7F0→ 5D0 transition. Inorganica Chim Acta 267:63–72
43. Latva M, Takalo H, Mukkala VM, Matachescu C, Rodríguez-Ubis JC, Kankare J (1997) Correlation between the lowest triplet state energy level of the ligand and lanthanide(III) luminescence quantum yield. J Lumin 75:149–169. https://doi.org/10.1016/S0022-2313(97)00113-0